

# Genetic and biochemical characterization of an $\alpha$ -L-arabinofuranosidase isolated from a compost starter mixture

Kurt Wagschal<sup>\*</sup>, Diana Franqui-Espiet, Charles C. Lee, Rena E. Kibblewhite-Accinelli,  
George H. Robertson, Dominic W.S. Wong

USDA Agricultural Research Service, Western Regional Research Center, 800 Buchanan Street, Albany, CA 94710, United States

Received 17 November 2005; received in revised form 18 May 2006; accepted 14 June 2006

## Abstract

Enzymes that are involved in the breakdown of arabinoxylan biomass are becoming more important as the need to harness renewable energy sources becomes necessary. A gene encoding an  $\alpha$ -L-arabinofuranosidase not previously described (1581 bp) was isolated from a culture seeded with a compost starter mixed bacterial population. Sequence analysis of the putative catalytic domain determined that the enzyme, termed deAFc, is a glycoside hydrolase family 43 member. The gene was cloned into *Escherichia coli* with a C-terminal His-tag and its recombinant product expressed and purified. deAFc appeared to be monomeric under the gel-permeation chromatography conditions employed, and kinetic analysis using several artificial glycoside substrates revealed  $K_m$  values between 0.251 and 0.960 mM and  $k_{cat}$  values between 0.13 and 1.22 s<sup>-1</sup>. The purified enzyme was stable up to 45 °C, had an activity temperature optimum of 47 °C, and a pH profile that was essentially invariant between pH 5 and 8.5. deAFc was observed to release xylose only when incubated with synthetic xylopyranoside substrates, while release of arabinose was observed from arabinoxylan and branched arabinan as well as from synthetic chromophore or fluorophore-tagged  $\alpha$ -L-arabinofuranoside substrates.

© 2006 Elsevier Inc. All rights reserved.

**Keywords:** Arabinofuranosidase; Glycoside hydrolase family 43; Compost; Substrate inhibition; Hemicellulose degradation

## 1. Introduction

Enzymes that can be harnessed for the breakdown of hemicellulose in cereal crops and crop fiber biomass are becoming increasingly important due to their pivotal role in the utilization of these renewable energy sources. Hemicelluloses (xylans, arabinoxylans) are widely found as structural components in plant cell walls, where they cross-link with lignin and are extensively hydrogen-bonded to cellulose [1]. Structurally, xylans are heteropolysaccharides consisting of a linear  $\beta$ -D-(1 → 4)-linked xylopyranoside backbone that depending on the tissue source is variously substituted with arabinose and other substituents. The xylose backbone of cereal xylans can be substituted with (1 → 2)- and/or (1 → 3)-linked  $\alpha$ -L-arabinofuranosyl,  $\alpha$ -D-glucuronic acid, and O-2- and/or O-3-linked acetate groups. Moreover, the arabinofuranose residues can be esterified with ferulate and *p*-coumarate residues, which may in turn be cross-linked or oxidatively coupled to lignin.

Numerous enzymes with the ability to hydrolyze the various hemicellulose linkages have been isolated, most of them from microbial sources [2]. Enzymes that hydrolyze non-reducing terminal  $\alpha$ -L-arabinofuranosidic linkages and release arabinose in an *exo*-manner from substrates such as arabinoxylan, arabinan and from synthetic substrates such as *p*-nitrophenyl- $\alpha$ -L-arabinofuranoside (*p*-NP-AraF) are classified as  $\alpha$ -L-arabinofuranosidases (AFase, EC 3.2.1.55) [2,3]. AFase's and their potential biotechnological application have been the subject of several valuable reviews [2–5]. This class of enzymes is important since removal of the arabinose residues from the xylan backbone can have a synergistic effect with endoxylanase hydrolysis, presumably because endoxylanase hydrolysis of glycosidic bonds is inhibited by arabinose-substituted xylose residues [6,7]. In addition to the breakdown of hemicellulosic biomass for fuel and chemical feedstock use [5], AFase's may also find use in cellulose pulp biobleaching processes [8] and for the release of glycosidically bound monoterpene flavor constituents in grape juice [9]. We describe here the isolation of DNA from a culture seeded with a commercial compost starter, and the subsequent identification, cloning, expression, purification and genetic and biochemical

<sup>\*</sup> Corresponding author. Tel.: +1 510 559 6453; fax: +1 510 559 5940.  
E-mail address: [kwagschal@pw.usda.gov](mailto:kwagschal@pw.usda.gov) (K. Wagschal).

characterization of an encoded  $\alpha$ -L-arabinofuranosidase termed deAfc.

## 2. Materials and methods

### 2.1. Genomic DNA preparation

Dr. Earth compost starter (Dr. Earth Company, Los Angeles, CA) containing *B. subtilis*, *B. cereus*, *B. megaterium*, *Azobacter vinelandii*, *Rhizobium japonicum* and *Lactobacillus acidophilus* was used to inoculate a minimal media liquid culture (EZ Rich defined media; Teknova, Hollister, CA) supplemented 0.67% (w/v) each of xylan from birch wood, beech wood, and oat spelt (Sigma, St. Louis, MO, USA). The culture was grown overnight at 30 °C and 200 rpm. Cells were isolated by centrifugation, and genomic DNA was isolated from the cell pellet using the FastDNA Kit (Qbiogene, Irvine, CA) with Lysing Matrix 2 and CLS-TC solution according to manufacturer's protocol.

#### 2.1.1. Genomic library construction and activity screening

Genomic DNA isolated from the Dr. Earth compost starter was partially digested with *ApoI* restriction enzyme. The digest was separated using agarose gel electrophoresis, and fragments 4–10 kb were excised and purified using the QiaExII gel purification kit (Qiagen, Valencia, CA). These fragments were then ligated to an *EcoRI*-digested Lambda ZAP II vector and packaged into lambda phage using Lambda ZAP II Vector and Gigapack III Packaging Extract (Stratagene, La Jolla, CA, USA). XL1-Blue MRF' cells (Stratagene) were infected with the phage genomic DNA library and spread onto NZY (0.5% sodium chloride, 0.2% magnesium sulfate heptahydrate, 0.5% yeast extract, 1% casein hydrosylate, and 1.5% agar) media plates. The infection was overlaid with agarose containing 4-*O*-methyl-D-glucurono-D-xylan-remazol brilliant blue R (RBB-xylan; Megazyme, Bray, Ireland). Clearings in the RBB-xylan overlay indicated the presence of phage plaques encoding xylan-degrading genes. The plaques were isolated and purified by repeated screenings on RBB-xylan. Single-clone excision was conducted according to manufacturer's protocol (Stratagene) to obtain a pBS-SK construct with an inserted fragment of genomic DNA.

#### 2.1.2. Sub-cloning of the deAfc gene

A cloned fragment of genomic DNA was sequenced in its entirety. An open reading frame encoding a putative glycosyl hydrolase family 43 AFase was discovered using the VectorNTI software package (Invitrogen, Carlsbad, CA, USA) and BLAST analysis [10]. The gene was isolated by PCR using the following primers which contained linkers encoding *NdeI* and *XhoI* restriction enzyme sites (underlined) on the 5' and 3' primers, respectively:

- deAfc-5': CGCCATATGAAATTTCTAAATCCTGTTATACCCGGTTTTC
- deAfc-3': GCGCTCGAGTTGTTCTAAATATTATACAGAAACCTCAGT-CACATTAA

The amplified gene and the pET-22b(+) plasmid (EMD Biosciences, San Diego, CA, USA) were digested with *NdeI* and *XhoI* restriction enzymes and ligated to create a pET22b(+)-deAfc expression vector with a C-terminal His-tag.

### 2.2. deAfc expression and purification

The expression host *E. coli* BL21(DE3) was transformed with the expression plasmid pET22b(+) containing the deAfc insert, streaked onto Luria–Bertani agar plates amended with 50  $\mu$ g/ml carbenicillin (Sigma) (LB<sub>carb</sub>), and incubated overnight at 37 °C. Positive transformants were selected based on enzymatic hydrolysis of *p*-NP-AraF (described below) and restriction digestion of the plasmids. A single positive transformant was used to inoculate a 15 ml seed culture of *E. coli*, which was then grown in LB<sub>carb</sub> broth at 37 °C at 250 rpm for 16 h with 0.5% glucose added to repress protein expression. A 5 ml aliquot was used to inoculate 200 ml LB<sub>carb</sub>, which was grown at 37 °C to OD<sub>600nm</sub> = 2–3. Then 1 mM IPTG was added to induce protein expression, and incubation was allowed to proceed at 16 °C at 250 rpm for 16 h. 50 ml aliquots were pelleted and the pellets stored frozen at –80 °C. Cell lysis and release of soluble proteins was achieved by adding to each pellet 3.5 ml Bug-Buster solution (EMD Biosciences) containing 40 U/ml *r*-Lysozyme (EMD Biosciences), 0.5 mM phenylmethylsulfonylfluoride (PMSF), 25 U/ml Benzonase, and 5 mM  $\beta$ -mercaptoethanol (BME; all from Sigma). Cells were incubated in the lysis solution for 20 min at room temperature, cooled to 0–4 °C and centrifuged to remove cell debris. The protein was purified using Ni-NTA resin (Qiagen) according to the manufacturer's instructions, by first adjusting the supernatant solution to 300 mM NaCl, 10 mM imidazole and 50 mM phosphate buffer (pH 8.0). The composition of the wash buffer used was 50 mM phosphate buffer (pH 8.0) containing 1 mM BME, 1  $\mu$ l/ml protease inhibitor cocktail III (EMD Biosciences), 300 mM NaCl and 10 mM imidazole. The protein was eluted using the same buffer except that the imidazole concentration was increased to 250 mM. Fractions containing the enzyme were buffer exchanged using NAP-5 desalting columns (Amersham Biosciences, Piscataway, NJ) into 50 mM phosphate (pH 6.0), 10% glycerol and 200  $\mu$ M PMSF and stored at –80 °C. Protein concentrations were determined using Coomassie Plus reagent (Pierce Biotechnology, Rockford, IL, USA) following the manufacturer's protocol. Enzyme fractions were analyzed using PAGE following the manufacturer's protocol (Invitrogen). Final protein purity was estimated by gel densitometry performed using an AlphaImager imaging system (Alpha Innotech Corp., San Leandro, CA, USA).

### 2.3. Molecular weight determination

The molecular weight of the His-tagged protein was estimated by gel filtration chromatography using an Amersham/Pharmacia HiPrep 16/60 Sephacryl S-300 HR column (Amersham Biosciences). The running buffer was 50 mM phosphate (pH 8.0), 150 mM NaCl, 1 mM dithiothreitol (DTT), and 10% sucrose (w/v), and a standard curve was generated with low molecular weight (13.7–67 kDa) and high molecular weight (158–669 kDa) standards (Amersham Biosciences).

### 2.4. Enzyme assays

For assays using nitrophenyl (NP) glycosides as substrates (all from Sigma), the enzyme activity was determined by measuring the change in absorbance at 400 nm due to NP release using a Spectramax M2 spectrophotometer equipped with a temperature controller (Molecular Devices, Sunnyvale, CA, USA). Time course studies using saturating substrate concentrations were initially performed with *p*-NP-AraF to establish the linearity of hydrolysis rate with respect to time at 45 °C. In a typical kinetic assay 190  $\mu$ l of 50 mM phosphate (pH 8.0) containing

Table 1  
Kinetic parameters for synthetic substrate hydrolysis<sup>a</sup>

Substrate	Concentration range ( $\mu$ M)	$K_m$ ( $\mu$ M)	$k_{cat}$ ( $s^{-1}$ )	$k_{cat}/K_m$ ( $mM^{-1} s^{-1}$ )
<i>p</i> -NP-AraF	30–4000	251 $\pm$ 11.8	0.684 $\pm$ 0.009	2.73 $\pm$ 0.133
<i>p</i> -NP-XylP	15–4000	960 $\pm$ 42.6	0.132 $\pm$ 0.003	0.138 $\pm$ 0.007
<i>o</i> -NP-XylP	30–7000	766 $\pm$ 41	1.22 $\pm$ 0.02	1.59 $\pm$ 0.09
4-MU-XylP <sup>b</sup>	10–4000	712 $\pm$ 66	0.571 $\pm$ 0.033	0.802 $\pm$ 0.088

<sup>a</sup> Results shown were obtained at pH 8.0. At pH 5.0 the kinetic parameters were  $K_m = 0.600 \pm 54 \mu$ M,  $k_{cat} = 0.461 \pm 0.025 s^{-1}$  and  $k_{cat}/K_m = 0.768 \pm 0.081$ .

<sup>b</sup> Reaction conditions were as described in the text.

0.1% bovine serum albumin (BSA; Sigma) and varying substrate concentrations was pre-incubated at 45 °C for 5 min, then 10 µl enzyme solution was added and mixed to initiate the reaction. Generally, sixteen different substrate concentrations were used to assess the kinetic parameters (Table 1), and the amount of enzyme was chosen so that the proportion of substrate hydrolyzed at the end of the data acquisition period ranged from 1 to 3% (29 nM deAFc for *p*-NP-AraF and 114 nM deAFc for *o*- and *p*-nitrophenyl-β-D-xylopyranoside (*o*- and *p*-NP-XylIP)). The kinetic parameters  $V_{\max}$  and  $K_m$  for the aryl-glycoside substrates (Table 1) were calculated by non-linear regression fitting of the data to the Michaelis–Menten equation using the program GraFit 5 (Erithacus Software, Surrey, UK). The inhibition constant  $K_i$  for arabinose was determined using a kinetic spectrophotometric assay wherein velocity was measured in the absence of added arabinose, and then in the presence of 30, 60 and finally 120 mM arabinose using *p*-NP-AraF concentrations ranging from 120 to 4000 µM, 50 mM PO<sub>4</sub> (pH 8.0) and 33.3 nM deAFc. Arabinose at the various concentrations and deAFc were pre-incubated in the assay buffer for 10 min at 45 °C, and the reaction initiated by adding the substrate. Kinetic parameters were obtained by non-linear curve fitting of the data to a competitive inhibition model using GraphPad Prism 4 (GraphPad Software, San Diego, CA, USA).

## 2.5. Activity versus pH profile

The effect of pH on the apparent  $V_{\max}$  (Fig. 1) was measured using endpoint assays utilizing an equal volume of 1 M Na<sub>2</sub>CO<sub>3</sub> to quench the reactions and raise all the pH values to ~pH 11. Reactions were carried out at 45 °C using saturating concentrations of either *p*-NP-AraF (4 mM) or *p*-NP-XylIP (6.4 mM), 372 nM deAFc, 0.1% BSA, and incubation for 17–25 min at 45 °C, followed by quenching with an equal volume of 1 M Na<sub>2</sub>CO<sub>3</sub> and absorbance measurement at 400 nm. The pH profiles were obtained using multi-component buffers and both substrates in separate experiments. For pH 3–8, 50 mM McIlvaine buffer (50 mM citrate, 50 mM phosphate) was employed, while for pH 8–11 a universal buffer consisting of 50 mM citrate, 50 mM phosphate and 50 mM borate was used. The pH curve was also generated with *p*-NP-AraF and the single component buffers 100 mM citrate for pH 3–6.5, 100 mM phosphate for pH 6.5–8.0, and 100 mM AMPSO for pH 8.0–9.5. Reaction was allowed to proceed for 17 min (maximum of 10% substrate depletion) when using *p*-NP-AraF, or for 25 min (maximum 5% substrate depletion) when using *p*-NP-XylIP as the substrate. To confirm substrate saturation at the pH extremes, the substrate 4-methyl-umbelliferyl-β-D-xylopyranoside (4-MU-XylIP, Sigma) was used to assess the kinetic parameters at both pH 5 and 8 (Table 1) because unlike nitrophenyl, the fluorescent 4-MU group can be readily detected at pH 5. An excitation wavelength of 349 nm and an emission wavelength of 460 nm was used to quantify 4-MU release at both pH 5 and 8. Reaction conditions were 45 °C, 29 nM deAFc, 10–4000 µM 4-MU-XylIP, 100 mM citrate for pH 5.0 or 100 mM AMPSO for pH 8.0 and 0.1%

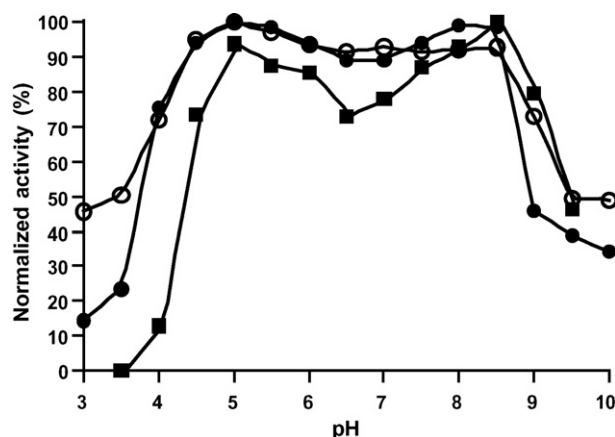


Fig. 1. Relative enzyme activity at the indicated pH values. McIlvaine's buffer was used for pH 3–8, and universal buffer was used for pH 8–11. Enzyme activity was determined with 4 mM *p*-NP-AraF (●) or 6.4 mM *p*-NP-XylIP (○). The pH profile was also generated using 4 mM *p*-NP-AraF and single component buffers (■). Reaction conditions were as described in Section 2.

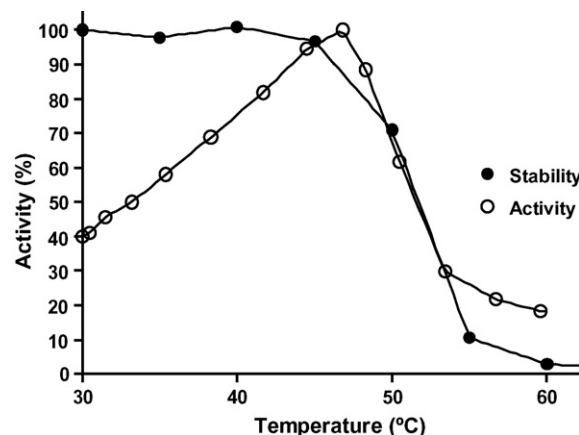


Fig. 2. Enzyme stability at the indicated temperatures (●), and enzyme activity (relative  $V_{\max}$ ) at the indicated temperatures (○). Reaction conditions were as described in Section 2.

BSA. The kinetic parameters  $V_{\max}$ ,  $K_m$  and  $K_i$  were calculated by non-linear regression fitting of the data to Eq. (1), derived from a substrate uncompetitive inhibition model [11], using GraphPad Prism 4 (GraphPad Software):

$$v_0 = \frac{k_{\text{cat}} \times [E_0] \times [S]}{K_m + [S] + ([S]^2/K_i)} \quad (1)$$

## 2.6. Activity versus temperature and thermostability profiles

The effect of temperature on enzyme stability (Fig. 2) was determined by first measuring the rate of *p*-NP-AraF hydrolysis prior to thermal challenge. Reaction conditions were 45 °C, 50 mM HPO<sub>4</sub> (pH 8.0), 0.1% BSA, 6.4 mM *p*-NP-AraF, and 47 nM deAFc. Then aliquots of the enzyme solution were transferred to a 96-well PCR plate and subjected to incubation at a series of temperatures ranging from 30 to 70 °C for 5 min using a temperature gradient PCR machine (MJ Research, Watertown, MA, USA). After thermal treatment the enzyme activity was again measured to allow calculation of the residual activity. Eight data points were obtained for each temperature tested, and the residual activity normalized to the highest recorded initial activity.

The effect of temperature on the apparent  $V_{\max}$  was determined by performing endpoint assays using the same reaction conditions as used for the enzyme thermal stability experiments. deAFc was incubated for 30 min at the various temperatures under saturating substrate concentrations, quenched with an equal volume of 1 M Na<sub>2</sub>CO<sub>3</sub>, and *p*-NP release quantitated at 400 nm using a standard curve generated on the same microtiter plate.

## 2.7. Substrate specificity

The ability of deAFc to hydrolyze the natural substrate xylobiose (Table 2) was assessed using 800 nM deAFc and substrate concentrations of 100 µM to 9 mM, 100 mM phosphate buffer (pH 8), and a 60 min incubation at 45 °C. Enzyme activity resulting in xylose release was then assessed using an enzyme-coupled assay for xylose as described [12]. TLC was used to monitor the degradation of the following natural polymeric substrates: sugar beet arabinan, debranched sugar beet arabinan, rye arabinoxylan, wheat medium viscosity arabinoxylan (all from Megazyme), birchwood xylan, beechwood xylan, oat-spelt

Table 2  
deAFc substrate specificity

Substrate	Specific activity (µmol/mg min)	Normalized activity (%)
<i>p</i> -NP-AraF	0.6829	100
<i>p</i> -NP-XylIP	0.0792	11
<i>o</i> -NP-XylIP	0.9966	146

xylan and larchwood (+)-arabinogalactan (all from Sigma). The sugar beet arabinan substrate consisted of a 1,5- $\alpha$ -linked arabinose backbone to which 1,3- $\alpha$ -linked and possibly some 1,2- $\alpha$ -linked L-arabinofuranosyl groups were attached. Approximately 60% of the main-chain arabinofuranosyl residues were substituted by single 1,3-linked arabinofuranosyl groups. The debranched sugar beet arabinan was prepared by the manufacturer such that all 1,2- and 1,3- $\alpha$ -linked L-arabinofuranosyl branch units were removed. The cereal grain natural arabinoxylan substrates had homopolymeric backbones of (1-4)- $\beta$ -D-xylopyranosyl residues substituted with (1-2)- and/or (1-3)- $\alpha$ -linked L-arabinofuranosyl branch units. The wheat arabinan medium viscosity arabinoxylan (Megazyme) had an arabinose:xylose:other sugars ratio of 37:61:2. The rye flour arabinoxylan (Megazyme) had a sugar composition of arabinose:xylose:other sugars of 49:48:3. The oat-spelt xylan used contained minimally 70% xylose and maximally 10% arabinose and 15% glucose. The xylans from the two hardwoods birchwood and beechwood were also tested, were each specified as containing >90% xylose residues. Reaction conditions were overnight incubation at 37 °C in 100 mM phosphate (pH 8.0) containing 1  $\mu$ l/ml protease inhibitor cocktail III, 5 mM DTT, 0.1% BSA, polymeric substrate concentrations between 0.9 and 2.2 mg/ml and 2.9  $\mu$ M deAFc. TLC was performed using HPTLC silica plates (Alltech, Waukegan, IL, USA), with mobile phase composition EtOAc:MeOH:H<sub>2</sub>O of 7:2:1. Detection was performed using 20% H<sub>2</sub>SO<sub>4</sub> in MeOH with 1 mg/ml orcinol (Aldrich).

Action on the following artificial aryl-glycoside substrates was tested (Table 2): *p*-NP- $\alpha$ -L-arabinofuranoside, *p*-NP- $\alpha$ -L-arabinopyranoside, *p*-NP- $\beta$ -D-xylopyranoside, *o*-NP- $\beta$ -D-xylopyranoside, *p*-NP- $\beta$ -D-glucopyranoside, *p*-NP- $\beta$ -D-fucopyranoside, *p*-NP- $\beta$ -D-galactopyranoside, and *p*-NP- $\beta$ -D-mannopyranoside (all from Sigma). Reaction conditions were 45 °C, 29 nM deAFc, 4 mM aryl-glycoside substrate, 50 mM phosphate buffer (pH 8.0). Nitrophenyl group release was monitored by measuring the change in absorbance at 400 nm.

### 3. Results and discussion

#### 3.1. Sequence analysis

The AFase's from several bacterial species have been characterized, and based on amino acid sequence similarity have been classified into glycoside hydrolase (GH) families 3, 43, 51, 54, 62 and 93 of the CAZy classification (P.M. Coutinho and B. Henrissat, <http://afmb.cnrs-mrs.fr/CAZY>) [13]. The gene encoding the AFase termed deAFc (1581 bp, GenBank accession no. DQ284779) was sequenced from a phage DNA library clone that exhibited xylanase activity on the dye-labeled substrate RBB-xylan. The phage clone contained a 3511 bp genomic DNA insert, and BLAST analysis revealed three putative open reading frames on the same coding strand in the following arrangement: partial sequence of an ABC-type sugar transport system permease component (ABC-permease), a GH family 10 xylanase (GH10 Xyn) and a GH family 43 arabinofuranosidase/xylosidase (deAFc). Seventy-four nucleotides separated the predicted stop codon of the putative permease component and the translation start site of GH10 Xyn, and 168 bp separated the predicted stop codon of the GH10 Xyn and the translation start site of deAFc. Inspection of the sequences for bacterial promoters and rho-independent transcription termination sites was performed using BPROM and FindTerm, available at [www.softberry.com](http://www.softberry.com). Promoters were predicted to exist upstream of both GH10 Xyn and deAFc. The promoter for GH10 Xyn has a -10 box with a score of 65 and a -35 box with a score of 30, and the promoter for deAFc has a -10 box with a score of 65 and a -35 box with a score of 15

(scores are as given by BPROM). No rho-independent transcription termination sites were found in the regions upstream of the stop codons for either ABC-permease or GH10 Xyn, while for deAFc a potential site occurs at the end of the gene with a score of -14.5 (score as given by FindTerm). Thus, while the presence of multiple potential promoters suggests that GH10 Xyn and deAFc can be independently regulated, the proximity of the genes and their potential to coordinately assimilate carbon, coupled with the absence of identifiable transcription termination sites after ABC-permease and GH10 Xyn, leaves open the possibility that the cloned insert is part of a polycistronic operon. This would have precedence since the genes encoding the components of xylan-degradation pathways are known to be organized as operons in bacterial species [14].

Phylogenetic analysis of the evolutionary relationship of the amino acid sequence of deAFc to other GH's shows closest relationship to GH's from *Geobacillus thermoleovorans* (55% positive, 44% identical; NCBI accession 85717961), DNA isolated from uncultured anaerobic sediments from Baltimore Harbour (54% positive, 41% identical; NCBI accession 82524016 [15]), *Oceanobacillus iheyensis* HTE831 (51% positive, 39% identical; NCBI accession 23099542) [16], and *Bacillus clausii* KSM-K16 (51% positive, 39% identical; NCBI accession 56962920). These enzymes are all members of the GH family 43, and furthermore are predicted to have arabinofuranosidase or xylosidase activity. Thus, based on amino acid sequence deAFc belongs to GH family 43, which includes xylanases,  $\beta$ -D-xylosidases, arabinanases and  $\alpha$ -L-arabinofuranosidases.

The catalytic mechanism of hydrolysis is conserved for all members within a given sequence-based GH family [17,18], and has been reported to result in inversion of the anomeric center in three independent studies of GH family 43 glycohydrolases [19–21]. In the case of inverting hydrolytic enzymes, a single-displacement reaction ensues [22], and for GH's one active-site carboxylate provides general base catalytic assistance to the attack of water, while another carboxylic acid provides general acid catalytic assistance to cleaving of the glycosidic bond [23]. deAFc is similar to a GH family 43  $\beta$ -D-xylosidase termed XynB3 from *Geobacillus stearothermophilus* T-6 (43% positive, 30% identical; NCBI accession 51235720), which has been extensively characterized and for which the catalytic active-site residues have been identified [24]. Alignment of the amino acid sequences of deAFc and XynB3 shows high homology around the active-site residues, with Asp14 predicted to be the general base (aligns with Asp 15 in XynB3) and Glu175 predicted to be the general acid residue (aligns with Glu187 in XynB3).

#### 3.2. Oligomerization state

After purification of the protein using Ni-NTA, protein purity was estimated to be 95% using gel densitometry. The protein deAFc eluted as a single peak during gel filtration chromatography coincident with *p*-NP-AraF hydrolytic activity (data not shown). The apparent  $M_W$  value of ~57.9 kDa obtained from the gel filtration experiment implies the protein eluted as a monomer under the conditions employed since the  $M_W$  value was within experimental error of the calculated subunit  $M_W$  of 60.1 kDa



based on the amino acid sequence predicted for expression of the His-tagged protein in *E. coli* by Vector NTI (Invitrogen). Other AFase's have molecular weights that are consistent with monomer, dimer and higher quaternary structures. For example, an AFase isolated from *Butyrivibrio fibrisolvens* was a homooctamer of 31 kDa subunits with an apparent  $M_W$  of 240 kDa [25], while a thermostable GH family 51 AFase from *Thermotoga maritima* was reported to be a hexamer [26].

### 3.3. Enzyme kinetic parameters

Time course studies initially performed established that the rate of *p*-NP-AraF substrate hydrolysis under saturating conditions was linear with respect to time ( $R^2 > 0.99$ ) for at least 90 min at 45 °C. The Michaelis–Menten parameters for hydrolysis of *p*-NP-AraF, *o*- and *p*-NP-XylP and 4-MU-XylP are shown in Table 1. The  $K_m$  values were all of the same order of magnitude, and ranged from  $\sim 250 \mu\text{M}$  for *p*-NP-AraF to  $\sim 960 \mu\text{M}$  for *p*-NP-XylP. The  $k_{\text{cat}}$  values were all within one order of magnitude, ranging from  $\sim 0.13 \text{ s}^{-1}$  for *p*-NP-XylP to  $1.22 \text{ s}^{-1}$  for *o*-NP-XylP. Interestingly, while the  $K_m$  values for *o*- and *p*-NP-XylP were similar, the ratio  $k_{\text{cat}} \text{ } o\text{-NP-XylP}/k_{\text{cat}} \text{ } p\text{-NP-XylP}$  was  $\sim 9$  even though the  $\text{p}K_a$ 's of the leaving groups are similar (7.22 for *o*-NP and 7.18 for *p*-NP). Contributing significantly to the observed difference hydrolysis rate of *o*- and *p*-NP-XylP are differences in the noncovalent enzyme/substrate interactions (e.g. hydrogen bonding) of these stereoelectronically different leaving groups in the active site and the attendant differences in stabilization of their respective oxocarbenium ion-like transition states [27]. Thus, results similar to deAFc have previously been reported for a GH family 52  $\beta$ -xylosidase, where  $k_{\text{cat}} \text{ } o\text{-NP-XylP}/k_{\text{cat}} \text{ } p\text{-NP-XylP}$  was  $\sim 4$  while  $K_m$  values were similar [28]. On the other hand, similar  $k_{\text{cat}}$  values for *o*- and *p*-NP-XylP hydrolysis have been reported for a GH family 39  $\beta$ -xylosidase [29].

deAFc clearly showed the greatest specificity  $k_{\text{cat}}/K_m$  when *p*-NP-AraF was used as the substrate, being 2–20 times greater than for any of the other artificial substrates. Lineweaver–Burke plots of the data for the substrates in Table 1 (data not shown) indicated no deviation from Michaelis–Menten kinetics at the substrate concentrations tested, which can otherwise indicate that transglycosylation is affecting a rate-limiting step. The  $k_{\text{cat}}$  value of  $0.68 \text{ s}^{-1}$  measured for hydrolysis of *p*-NP-AraF by deAFc at 45 °C is  $\sim 32$ -fold lower than the  $k_{\text{cat}}$  values of  $22 \text{ s}^{-1}$  reported for hydrolysis of this substrate at 80 °C by a GH family 51 AFase from a thermophile [26], and 128-fold lower than the  $k_{\text{cat}}$  value of  $87 \text{ s}^{-1}$  reported for hydrolysis of this substrate at 40 °C by another GH family 51 AFase [30]. In contrast, the  $K_m$  value of 0.251 mM obtained for deAFc is from 1.7- to 2.6-fold lower. An estimate of the  $K_i$  for arabinose of 27 mM ( $R^2 = 0.99$ ; data not shown) was obtained from non-linear regression fitting of the data to a competitive inhibition model. There appears to be considerable variability in the susceptibility of arabinofuranosidases to product inhibition. For example, an AFase from the bacterial source *Butyrivibrio fibrisolvens* was not inhibited by up to 50 mM arabinose [25], and one from *Aureobasidium pullulans* was reported to not be inhibited by 1.2 M L-arabinose [31].

The substrate 4-MU-XylP elicited marked substrate inhibition at both pH 5 and 8, necessitating fitting of the data to Eq. (1), derived from a substrate uncompetitive inhibition kinetic scheme where an inactive  $\text{ES}_2$  ternary complex is formed due to unproductive binding of substrate. The  $K_i$ 's obtained at the two different pH's were the same within experimental error; the  $K_i$  for 4-MU-XylP at pH 5 was  $3.17 \pm 0.41 \text{ mM}$  ( $R^2 = 0.997$ ), and at pH 8 the  $K_i$  was  $3.77 \pm 0.53 \text{ mM}$  ( $R^2 = 0.997$ ). Stereoelectronic considerations may explain for the differing propensities of the *o*-NP-, *p*-NP- and 4-MU-XylP substrates to exhibit substrate inhibition. Previously, kinetic analysis of a GH family 51 AFase isolated from *Geobacillus stearothermophilus* T-6 (AbfA T-6) gave typical Michaelis–Menten curves with a series of aryl-arabinofuranosides including 2,5-dinitrophenyl- $\alpha$ -L-arabinofuranoside and *p*-NP-AraF. However, kinetics consistent with substrate inhibition was observed for the 3-NP analog ( $K_i = 10 \text{ mM}$ ) and 3,4-DNP analog ( $K_i = 12 \text{ mM}$ ) [30]. Substrate inhibition by xylotriase ( $K_i = 1.7 \text{ mM}$ ), and no inhibition by xylobiose, has previously been observed for a *Thermoanaerobacterium* sp. GH family 37  $\beta$ -D-xylosidase [12].

### 3.4. Substrate specificity

Examples of GH family 43 enzymatic activity include  $\beta$ -xylosidase (EC 3.2.1.37),  $\alpha$ -L-arabinofuranosidase (EC 3.2.1.55), arabinase (EC 3.2.1.99), xylanase (EC 3.2.1.8) and galactan 1,3- $\beta$ -galactosidase (EC 3.2.1.145) (P.M. Coutinho and B. Henrissat, <http://afmb.cnrs-mrs.fr/CAZY>) [13]. It has also been shown that within a given class these enzymes show discrimination between natural and artificial substrates [32]. Thus, in order to accurately assign the substrate specificity of deAFc, a series of artificial and natural substrates were tested. deAFc was able to cleave both the arabinofuranosyl and xylopyranosyl synthetic aryl substrates, while no activity was detected with the other aryl-glycoside synthetic substrates (Table 2). D-Xylopyranose and L-arabinofuranose are spatially similar, thereby rationalizing the bifunctional  $\alpha$ -L-arabinofuranosidase/ $\beta$ -D-xylosidase activity of deAFc with respect to hydrolysis of synthetic substrates containing the relatively good leaving groups *o*-NP ( $\text{p}K_a$  7.22), *p*-NP ( $\text{p}K_a$  7.18) or 4-MU ( $\text{p}K_a$  8.2). In the natural substrate, however, the leaving groups are either xylose or arabinose moieties, which are very poor leaving groups with  $\text{p}K_a$ 's  $> 12$ . When hydrolysis of natural substrate glycosidic bonds by deAFc was tested, only release of arabinose (and not xylose) was observed by TLC from rye, wheat and oat-spelt arabinoxylan. The natural xylooligosaccharide substrate xylobiose was not hydrolyzed by the enzyme. Also, it was found that deAFc released arabinose from sugar beet arabinan containing (1-3)- $\alpha$ -linked L-arabinofuranosyl branch units, while no activity was detected on the corresponding debranched 1,5- $\alpha$ -linked arabinan polymer. While no hydrolysis products were detected for the substrates birchwood xylan or beechwood xylan, this is not surprising since deAFc appears unable to hydrolyze xylopyranoside linkages, and it has been reported that these hardwood xylans contain little or no arabinofuranosyl substitution [33]. Also, no hydrolysis products were detected for larchwood (+)-arabinogalactan even

though the ratio of arabinose:xylose units has been reported to be 11:56 for this substrate [34]. These results provides some information about possible linkage hydrolysis regio-specificity since arabinose in larchwood (+)-arabinogalactan is mainly *O*-2 linked to xylose, whereas in oat-spelt xylan the arabinofuranosyl units are mainly *O*-3 linked [34]. With respect to natural substrate specificity, it can be concluded that deAFc is specific for hydrolyzing arabinofuranosyl units, and the results further suggest deAFc may be specific for hydrolysis of (1-3)- $\alpha$ -L-arabinofuranosyl branch units. These results are in accord with previous studies where it has been shown that AFase's usually have a narrow range of substrate specificity [32,35]. The deAFc substrate specificity reported here is similar to that of an AFase from *Streptomyces lividans*, where a preference for arabinoxylans from cereal grains was observed, and no hydrolysis was observed with birchwood xylan, larchwood xylan, arabinogalactan or linear  $\alpha$ -1,5-arabinan [36].

### 3.5. pH curve

Broad pH/activity profiles were obtained showing essentially invariant  $V_{\max}$  values between pH 5 and 8.5, resulting in an activity plateau save a slight dip around pH 7. These results were reproducibly obtained using either multi-component or single-component buffers, and using either *p*-NP-AraF or *p*-NP-XylP as substrate (Fig. 1). Values of  $K_m$  and  $k_{\text{cat}}$  were subsequently determined at pH 5 and 8, corresponding to approximate activity maxima at low and high pH, to verify that saturating conditions were maintained throughout the pH range assayed. Kinetic spectrophotometric assays were performed with the synthetic substrate 4-MU-AraF since the 4-MU released can be detected fluorometrically in kinetic assays at both pH 5 and 8, while the extinction coefficient of *p*-NP is too low at pH 5 to allow for its use. It was found that identical  $K_m$  values and similar  $k_{\text{cat}}$  values were obtained within experimental error at the low and high pH extremes (Table 1). This observed identity at pH 5 and 8 of the kinetic parameters indicates that the broad pH curve is not a result of an artifact influencing the measured  $V_{\max}$  values, and is truly due to active-site invariance of activity with respect to pH over the range pH 5–8.5. (Fig. 1). This suggests that deAFc may not require general acid catalytic assistance to hydrolyze the relatively good leaving groups *p*-NP ( $\text{p}K_a$  7.18) or 4-MU ( $\text{p}K_a$  7.80) of the synthetic substrates used to generate the pH curves. Thus, it has previously been shown that for hydrolysis of 2,4-dinitrophenyl-cellobiose by wild-type  $\beta$ -1,4-glycanase from *Cellulomonas fimi*,  $k_{\text{cat}}$  was pH independent over the range pH 4.6–8.4, indicating no active-site ionizations which affects 2,4-dinitrophenyl-cellobiose hydrolysis rates occur in this pH range [37]. It is possible that for deAFc and other similar enzymes characterized using synthetic substrates, the broad pH profiles obtained would not extend to substrates with significantly higher leaving groups  $\text{p}K_a$ 's that demand participation of the acid catalyst carboxylate residue.

### 3.6. Thermal stability and $T_{\max}$

The enzyme was stable for 90 min up to 45 °C, whereupon the activity decreased rapidly to ~10% after only 5 min at 55 °C

(Fig. 2). The temperature maxima ( $T_{\max}$ ) was found to be 47 °C in 30 min endpoint assays, whereupon activity rapidly diminished, possibly due to enzyme thermal instability.

## 4. Conclusion

The gene encoding deAFc was isolated from a mixed bacterial culture obtained from a commercial compost starter mixture, and is classified as a GH family 43 member based on amino acid sequence. The enzyme was cloned with a C-terminal His tag, and the oligomerization state of the purified enzyme shown to be monomeric under the size-exclusion chromatography conditions employed. The enzyme showed a broad pH profile, with the activity being essentially invariant between pH 5 and 8.5. deAFc was not particularly heat stable, with stability decreasing rapidly at 55 °C, and a temperature maxima of 47 °C. While the enzyme was able to hydrolyze the artificial substrates *p*-NP-AraF, *o*-NP-XylP, *p*-NP-XylP and 4-MU-XylP, a clear preference for *p*-NP-AraF was observed based on  $k_{\text{cat}}/K_m$  values. Interestingly, testing substrate specificity using natural arabinoxylan substrates showed that arabinose was the only monosaccharide produced, and results were obtained consistent with the enzyme having a *O*-3-linked arabinose debranching activity.

## Acknowledgements

We gratefully acknowledge the many helpful corrections and suggestions of the reviewers. Reference to a company and/or products is for purposes of information and does not imply approval or recommendation of the product to the exclusion of others which may also be suitable. All programs and services of the U.S. Department of Agriculture are offered on a non-discriminatory basis without regard to race, color, national origin, religion, sex, age, marital status, or handicap.

## References

- [1] Bajpai P. Microbial xylanolytic enzyme system: properties and applications. *Adv Appl Microbiol* 1997;43:141–95.
- [2] Shallom D, Shoham Y. Microbial hemicellulases. *Curr Opin Microbiol* 2003;6:219–28.
- [3] Saha BC.  $\alpha$ -L-Arabinofuranosidases: biochemistry, molecular biology and application in biotechnology. *Biotechnol Adv* 2000;18:403–23.
- [4] Numan MT, Bhosle NB.  $\alpha$ -L-Arabinofuranosidases: the potential applications in biotechnology. *J Ind Microbiol Biotechnol* 2006;33:247–60.
- [5] Saha BC. Hemicellulose bioconversion. *J Ind Microbiol Biotechnol* 2003;30:279–91.
- [6] Rahman AKMS, Sugitani N, Hatsu M, Takamizawa K. A role of xylanase,  $\alpha$ -L-arabinofuranosidase, and xylosidase in xylan degradation. *Can J Microbiol* 2003;49:58–64.
- [7] Sørensen HR, Pedersen S, Viksø-Nielsen A, Meyer AS. Efficiencies of designed enzyme combinations in releasing arabinose and xylose from wheat arabinoxylan in an industrial ethanol fermentation residue. *Enzyme Microb Technol* 2005;36:773–84.
- [8] Curotto E, Nazal A, Aguirre C, Campos V, Durán N. Enzymatic pretreatment of kraft pulps from *Pinus radiata* D Don with xylanolytic complex of *Penicillium canescens* (CPI) fungi. *Appl Biochem Biotechnol* 1998;73:29–42.
- [9] Clinche FL, Piñaga F, Ramón D, Vallés S.  $\alpha$ -L-Arabinofuranosidases from *Aspergillus terreus* with potential application in enology: induction, purification and characterization. *J Agric Food Chem* 1997;45:2379–83.

- [10] Altschul SF, Gish W, Miller W, Myers EW, Lipman DJ. Basic local alignment search tool. *J Mol Biol* 1990;215:403–10.
- [11] Vallmitjana M, Ferrer-Navarro M, Planell R, Abel M, Ausín C, Querol E, et al. Mechanism of the family  $\beta$ -glucosidase from *Streptomyces* sp.: catalytic residues and kinetic studies. *Biochemistry* 2001;40:5975–82.
- [12] Wagschal K, Franqui-Espiet D, Lee CC, Robertson GH, Wong DWS. Enzyme-coupled assay for  $\beta$ -xylosidase hydrolysis of natural substrates. *Appl Environ Microbiol* 2005;71(9):5318–23.
- [13] Coutinho PM, Henrissat B. Carbohydrate-active enzymes: an integrated database approach. In: Gilbert HJ, et al., editors. Recent advances in carbohydrate bioengineering. Cambridge: The Royal Society of Chemistry; 1999. p. 3–12.
- [14] Shulami S, Gat O, Sonenshein AL, Shoham Y. The glucuronic acid utilization gene cluster from *Bacillus stearothermophilus* T-6. *J Bacteriol* 1999;181(12):3695–704.
- [15] Nesbø CL, Boucher Y, Dlutek M, Doolittle WF. Lateral gene transfer and phylogenetic assignment of environmental fosmid clones. *Environ Microbiol* 2005;7(12):2011–26.
- [16] Takami H, Takaki Y, Uchiyama I. Genome sequence of *Oceanobacillus iheyensis* isolated from the Iheya Ridge and its unexpected adaptive capabilities to extreme environments. *Nucleic Acids Res* 2002;30(18):3927–35.
- [17] Davies G, Henrissat B. Structures and mechanisms of glycosyl hydrolases. *Structure* 1995;3:853–9.
- [18] Gebler J, Gilkes N, Claeysens M, Wilson D, Beguin P, Wakarchuk W, et al. Stereoselective hydrolysis catalyzed by related  $\beta$ -1,4-glucanases and  $\beta$ -1,4-xylanases. *J Biol Chem* 1992;267:12559–61.
- [19] Pitson SM, Voragen AGJ, Beldman G. Stereochemical course of hydrolysis catalyzed by arabinofuranosyl hydrolases. *FEBS Lett* 1996;398:7–11.
- [20] Braun C, Meinke A, Ziser L, Withers SG. Simultaneous high-performance liquid chromatographic determination of both the cleavage pattern and the stereochemical outcome of the hydrolysis reactions catalyzed by various glycosidases. *Anal Biochem* 1993;212:259–62.
- [21] Kersters-Hilderson H, Claeysens M, Doorslaer EV, Bruyne CKD. Determination of the anomeric configuration of D-xylose with D-xylose isomerases. *Carbohydr Res* 1976;47:269–73.
- [22] Koshland DE. Stereochemistry and mechanism of enzyme reactions. *Biol Rev* 1953;28:416–36.
- [23] Ly HD, Withers SG. Mutagenesis of glycosidases. *Annu Rev Biochem* 1999;68:487–522.
- [24] Shallom D, Leon M, Bravman T, Ben-David A, Zaide G, Belakhov V, et al. Biochemical characterization and identification of the catalytic residues of a family 43  $\beta$ -D-xylosidase from *Geobacillus stearothermophilus* T-6. *Biochemistry* 2005;44:387–97.
- [25] Hespell RB, O'Brian PJ. Purification and characterization of an  $\alpha$ -L-arabinofuranosidase from *Butyrivibrio fibrisolvens* GS113. *Appl Environ Microbiol* 1992;58:1082–8.
- [26] Miyazaki K. Hyperthermophilic  $\alpha$ -L-arabinofuranosidase from *Thermotoga maritima* MSB8: molecular cloning, gene expression, and characterization of the recombinant protein. *Extremophiles* 2005;9(5):399–406.
- [27] Zechel DL, Withers SG. Glycosidase mechanisms: anatomy of a finely tuned catalyst. *Accounts Chem Res* 2000;33:11–8.
- [28] Bravman T, Belakhov V, Solomon D, Shoham G, Henrissat B, Baasov T, et al. Identification of the catalytic residues in family 52 glycoside hydrolase, a  $\beta$ -xylosidase from *Geobacillus stearothermophilus* T-6. *J Biol Chem* 2003;278(29):26742–9.
- [29] Vocadlo DJ, Wicki J, Rupitz K, Withers SG. A case for reverse protonation: identification of Glu160 as an acid/base catalyst in *Thermoanaerobacterium saccharolyticum* beta-xylosidase and detailed kinetic analysis of a site-directed mutant. *Biochemistry* 2002;41(31):9736–46.
- [30] Shallom D, Belakhov V, Solomon D, Shoham G, Baasov T, Shoham Y. Detailed kinetic analysis and identification of the nucleophile in  $\alpha$ -L-arabinofuranosidase from *Geobacillus stearothermophilus* T-6, a family 51 glycoside hydrolase. *J Biol Chem* 2002;277(46):43667–73.
- [31] Saha BC, Bothast RJ. Purification and characterization of a novel thermostable  $\alpha$ -L-arabinofuranosidase from a color-variant strain of *Aureobasidium pullulans*. *Appl Environ Microbiol* 1998;64:216–20.
- [32] Beldman G, Schols HA, Pitson SM, Leeuwen MJFS-v, Voragen AGJ. Arabinans and arabinan degrading enzymes. *Adv Macromol Carbohydr Res* 1997;1:1–64.
- [33] Timell T. Wood hemicelluloses. Part I. *Adv Carbohydr Chem Biochem* 1964;19:247–99.
- [34] Kormelink FJM, Voragen AGJ. Degradation of different [(glucurono)arabino]xylans by a combination of purified xylan-degrading enzymes. *Appl Microbiol Biotechnol* 1993;38:688–95.
- [35] Van Laere KMJ, Beldman G, Voragen AGJ. A new arabinofuranohydrolase from *Bifidobacterium adolescentis* able to remove arabinosyl residues from double-substituted xylose units in arabinoxylan. *Appl Microbiol Biotechnol* 1997;47:231–5.
- [36] Vincent P, Shareck F, Dupont C, Morosoli R, Kluepfel D. New  $\alpha$ -L-arabinofuranosidase produced by *Streptomyces lividans*: cloning and DNA sequence of the *abfB* gene and characterization of the enzyme. *Biochem J* 1997;322:845–52.
- [37] MacLeod A, Tull D, Rupitz K, Warren RAJ, Withers SG. Mechanistic consequences of mutation of active site carboxylates in a retaining  $\beta$ -4-glycanase from *Cellulomas fimi*. *Biochemistry* 1996;35:13165–72.